First principles investigation of the electronic structure of La_2MnNiO_6: An insulating ferromagnet

S.F. Matar[a,*], M.A. Subramanian[b], A. Villesuzanne[a], V. Eyert[c], M.-H. Whangbo[d]

[a]Institut de Chimie de la Matière Condensée de Bordeaux, I.C.M.C.B-CNRS, University Bordeaux 1, F-33608 Pessac Cedex, France
[b]DuPont Central Research and Development, Experimental Station, E328/219, Wilmington, DE 19880-0328, USA
[c]Institut für Physik, Universität Augsburg, 86135 Augsburg, Germany
[d]Department of Chemistry, North Carolina State University, Raleigh, NC 27695-8204, USA

Abstract

Using first principles density functional theory (DFT) calculations based on the full-potential linearized augmented plane wave method (LAPW), we investigated the electronic and magnetic structures for the ferromagnetic and antiferromagnetic states of La_2MnNiO_6 and analyzed the site-projected density of states and electronic dispersion curves. Our calculations show that the ground state of La_2MnNiO_6 is ferromagnetic insulating with the magnetization in agreement with Hund's first rule and experimental findings.
© 2006 Elsevier B.V. All rights reserved.

1. Introduction and theoretical framework

In the context of the emerging field of spin electronics, it is desirable to have semiconducting materials with strong ferromagnetic behavior near room temperature. However, the search for such materials is a difficult task due to conflicting requirements in the crystal structure, chemical bonding and electronic properties of semiconductors and ferromagnetic materials. CrO_2 is an example of a metallic ferromagnet at room temperature used in high-density magnetic recording and has been extensively studied both experimentally and theoretically [1]. Recently, near room temperature ferromagnetism in La_2NiMnO_6 has been confirmed through neutron diffraction studies [2]. This system is a rare example of a ferromagnetic insulator in which the spins, electric charge and dielectric properties can be tuned by magnetic and/or electric field. The purpose of this work is to present a theoretical analysis of the electronic and magnetic properties of La_2NiMnO_6 on the basis of first

principles density functional theory (DFT) calculations using the full-potential linearized augmented plane wave (FP-LAPW) method implemented in the Wien2k program package [3]. The validity and the limits of such a treatment of strongly correlated oxide systems have been discussed by one of us in a recent review on magnetic oxides [4]. For the exchange-correlation potential accounting for many body interactions, we used the local (spin) density approximation (L(S)DA) parameterization scheme according to Ceperley and Alder [5] and the generalized gradient approximation (GGA) according to Perdew and Wang [6]. Brillouin-zone (BZ) integrals were carried out using the special k-point sampling of Monkhorst and Pack [7]. The difference in total energies is converged to below 0.002 eV per cell with respect to k-point integration and kinetic energy cut-off. Therefore the same matrix size (approximately 97 plane waves per atom) and BZ sampling were used in each of the total energy calculations. The k-point mesh was varied up to a size of 234 ($11 \times 11 \times 7$). This was found sufficient to achieve the desired accuracy within the reciprocal space, i.e., an energy difference $\Delta E \sim 10^{-4}$ eV per cell between two successive iterative cycles.

*Corresponding author. Tel.: 00 33 5 40002690; fax: 00 33 5 40002761.
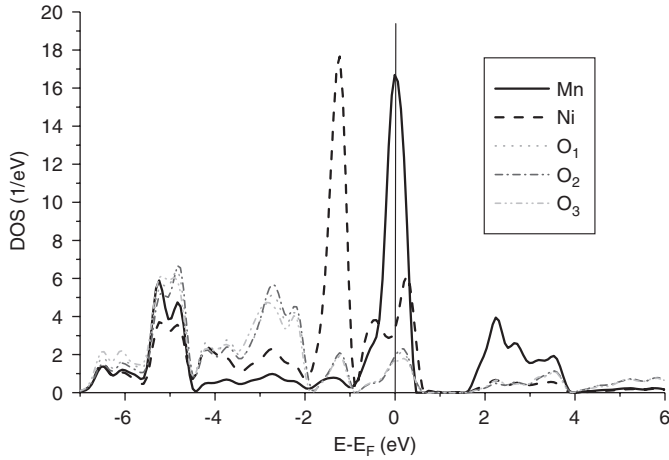E-mail address: matar@icmcb-bordeaux.cnrs.fr (S.F. Matar).

Fig. 1. Site-projected density of states in the non-magnetic state of La_2MnNiO_6. Empty La(4f) states above E_F are not shown for the sake of clarity.

Table 1
FP-LAPW calculated magnetic moments (inside atomic spheres) and energy difference for the ferromagnetic (F) and antiferromagnetic (AF) states of La_2MnNiO_6

La_2MnNiO_6	LSDA	GGA	Experimental
M (Mn/Ni) (μ_B)	F: 2.62/1.41	F: 2.64/1.46	F: Mn: 3
	AF: ±2.41/	AF: ±2.42/	Ni: 2
	±1.37	±1.45	
M (O/La) (μ_B)	F: 0.1/~0	F: 0.1/~0	—
	AF: 0	AF: 0	
M (total per formula unit) (μ_B)	F: 5	F: 5	~5
	AF: 0	AF: 0	
E(F)–E(AF) (eV per cell)	−0.15	−1.3	

2. Results and discussion

2.1. Search of magnetic instability: Non-spin-polarized (NSP) calculations

Firstly non-magnetic calculations enforcing spin degeneracy for all atomic sites were carried out. While this does not represent a paramagnetic situation, which would require heavy computations involving large supercells with random spin orientations, our objective here is to point out the possible magnetic instability on the different atomic sites before actual spin polarized (SP) calculations are done. The site-projected DOS are shown in Fig. 1; they are representative of two La_2MnNiO_6 units per cell ($Z = 2$). The valence band is dominated by oxygen states in the range from -7 to -2 eV; they mix with the lower part of Mn and Ni states. The Ni DOS are mainly below E_F while Mn states are found at the Fermi level (E_F) (t_{2g} states) and above E_F (empty e_g states). This picture is consistent with the expected oxidation states of Ni^{2+} (d^8) and Mn^{4+} (d^3). As a consequence, the DOS at E_F, $n(E_F)$, is significantly larger for Mn than for Ni. Within the Stoner theory of band ferromagnetism, which is a mean field approach, the large DOS at the Fermi level $n(E_F)$ is related to the instability of the non-magnetic state with respect to the onset of intraband spin polarization, when $n(E_F)I > 1$, where I is the Stoner integral, which was calculated and tabulated by Janak [8] for the elemental systems: I(Mn) = 0.408 eV and I(Ni) = 0.503 eV. With $n_{Mn}(E_F) = 8.5$ and $n_{Ni}(E_F) = 2$ eV^{-1} (per formula unit), the $n(E_F)I$ values are 3.47 and 1.06 for Mn and Ni, respectively. Note that the DOS magnitudes in Fig. 1 are relevant to two species of each, thus accounting for the stoichiometry
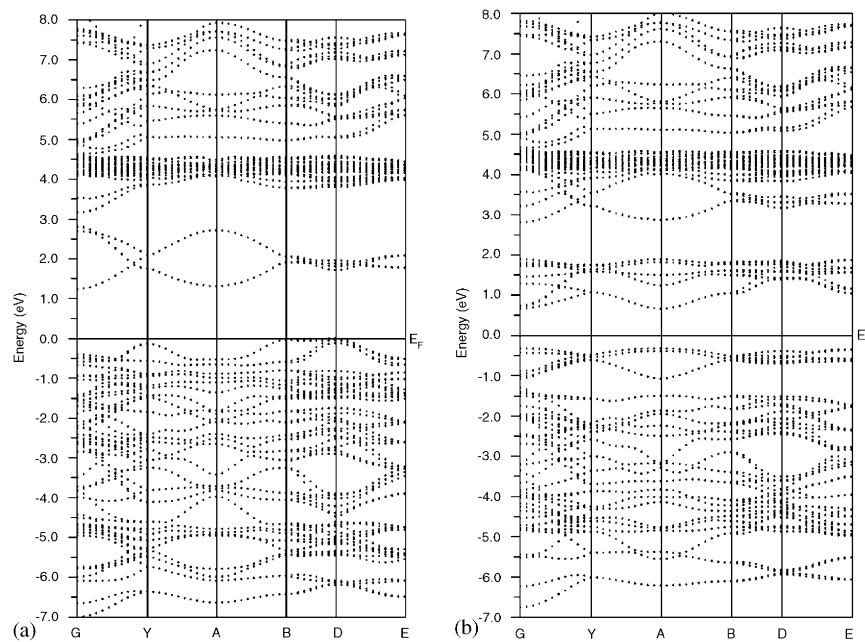

Fig. 2. Band dispersion for the ferromagnetic state of La_2MnNiO_6. (a) Spin ↑ bands and (b) spin ↓ bands along the main lines of the monoclinic BZ (G represents the Γ point of the BZ).

of the unit cell. This suggests that both the Mn and the Ni sites are magnetically unstable so that on-site magnetization should develop when SP calculations are carried out. Lastly, we note the relatively large DOS value of oxygen states at E_F, on which we comment in the next section devoted to SP calculations.

2.2. Spin polarized calculations of La$_2$NiMnO$_6$

Two magnetic states were considered for the search of the ground state: (i) the ferromagnetic state and (ii) the C-type antiferromagnetic state. The magnetic and crystallographic sublattices are the same in the ferromagnetic state, but are different in the antiferromagnetic state. The computations were again carried out to self consistency. Using LSDA as well as GGA functionals we arrive at the results shown in Table 1.

Although the atomic magnetic moments of Mn and Ni do not reach the experimental values, it is interesting to observe that the total magnetization per formula unit is 5 in agreement with experimental findings. This is due to the fact that there is a small amount of spin polarization on the oxygen atoms and in interstitial space such that the sum of the atomic moments of Ni, Mn and O leads to the integer value of 5. This value agrees with the Hund's first rule moments of Mn^{4+} (3d^3): t$_{2g}^3$ e$_g^0$ and Ni^{2+} (3d^8): t$_{2g}^6$ e$_g^2$. According to the Goodenough–Kanamori rule [9–11], the coupling between adjacent Mn^{4+} and Ni^{2+} sites should be ferromagnetic. This prediction is confirmed here, since both functional calculations show that the ferromagnetic state is more stable than the antiferromagnetic state, in agreement with the experiment [2]. In the following, we examine the electronic band structures in some detail.

An important feature of the ferromagnetic state is that it has a band gap of ∼1 eV and an insulating behavior for both ↑ (majority spins) and ↓ (minority spins) bands (Fig. 2). Among the empty conduction band, the La (4f) bands are flat and are found in the range 4–5 eV above E_F. Between these bands and E_F, the empty Mn (e$_g$↑) bands are found. All of the Mn (t$_{2g}$↑) bands lie below E_F and are responsible for the 3 μ_B moment, whereas the Ni (e$_g$↑) as well as the Ni (t$_{2g}$↑) bands are filled and lie below E_F. The panel of the minority spin bands is characterized by the empty Mn (t$_{2g}$↓), Mn (e$_g$↓) and Ni (e$_g$↓) bands between E_F and the La (4f) bands. The Ni (t$_{2g}$↓) bands occur within the valence bands. These features, which are illustrated in the Mn and Ni DOS plots of Figs. 3a and 3b, are fully consistent with the electronic structures expected from the oxidation formalism of Ni^{2+} and Mn^{4+}. The above analysis clearly shows different bonding behaviors of the two transition metal atoms in the majority and minority spin subbands. Such a feature of spin-dependent chemical bonding had been discussed before [4,12], and will be detailed further for this system in a forthcoming paper.
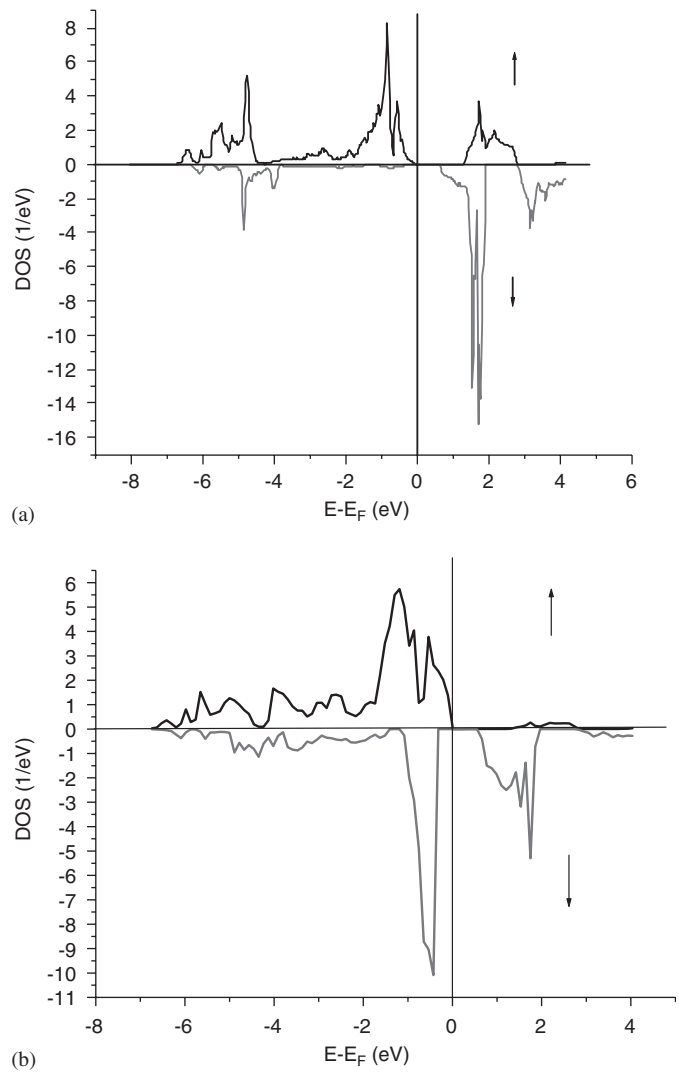

Fig. 3. Site and spin-projected DOS of Mn and Ni within La$_2$MnNiO$_6$ system.

3. Concluding remarks

The electronic band structure of La$_2$MnNiO$_6$ was investigated using DFT calculations with the purpose of assessing the magnetic ground state. Starting firstly from a non-magnetic calculation, the instability of the non-magnetic state is clearly shown according to the Stoner criterion of band ferromagnetism. Our SP calculations for the ferromagnetic and antiferromagnetic states with two exchange and correlation functionals (LSDA and GGA) show that the ferromagnetic state is the ground state from accurately computed energy differences. The total magnetization is ∼5 μ_B per formula unit and the band gap is close to ∼1 eV. This agrees with the available experimental observations. Our analyses strongly suggest a spin resolved chemical bonding. As a prospective, further investigations on chemical bonding versus magnetic ordering will be carried out.

Acknowledgments

References

[1] S. Matar, G. Demazeau, Chem. Phys. Lett. 407 (2005) 516.

[2] N.S. Rogado, J. Li, A.W. Sleight, M.A. Subramanian, Adv. Mater. 17 (2005) 2225.

[3] P. Blaha, K. Schwarz, G.K.H. Madsen, D. Kvasnicka, J. Luitz, Wien*2k*, An Augmented Plane Wave + Local Orbitals Program for Calculating Crystal Properties, Karlheinz Schwarz, Techn. Universität Wien, Austria, ISBN 3-9501031-1-2, 2001.

[4] S.F. Matar, Prog. Solid State Chem. 31 (2003) 239.

[5] D.M. Ceperley, B.J. Alder, Phys. Rev. Lett. 45 (1980) 1196.

[6] J.P. Perdew, Y. Wang, Phys. Rev. B 45 (1992) 13244.

[7] H.J. Monkhorst, J.D. Pack, Phys. Rev. B 13 (1976) 5188.

[8] J.F. Janak, Phys. Rev. B 16 (1977) 255.

[9] J.B. Goodenough, Phys. Rev. 100 (1955) 564.

[10] J.B. Goodenough, Phys. Chem. Solids 6 (1958) 287.

[11] J. Kanamori, Phys. Chem. Solids 10 (1959) 87.

[12] M.-H. Whangbo, H.-J. Koo, A. Villesuzanne, M. Pouchard, Inorg. Chem. 41 (2002) 1920.